Fields Institute Communications
Volume **36**, 2003

Interepidemic Intervals in Forced and Unforced SEIR Models

Chris Bauch
Department of Mathematics and Statistics
McMaster University
Hamilton, Ontario, Canada L8S 4K1
bauch@math.mcmaster.ca

David J.D. Earn
Department of Mathematics and Statistics
McMaster University
Hamilton, Ontario, Canada L8S 4K1
earn@math.mcmaster.ca

Abstract. Many infectious diseases give rise to recurrent epidemics. The time interval between epidemics is consequently an important property that epidemiologists and public health officials would like to be able to predict. Accurate estimates have been made for certain diseases by associating the observed interepidemic interval with the natural period of damped oscillations near the stable equilibrium solution of the standard (unforced) SEIR model. For childhood infections, this successful prediction is surprising because seasonal variation in contact rates (due to school terms) is known to have significant effects on patterns of disease incidence. Here, we show that the natural damping period of transients near the annual attractor of the seasonally forced SEIR model is usually well-approximated by the damping period obtained without forcing. This explains why naive calculations of interepidemic intervals have yielded accurate results in certain cases. However, the unforced approximation cannot be justified if the forced model has a non-annual attractor with a non-negligible basin of attraction, as is typically the case for measles; consequently, agreement between the interepidemic interval predicted by the unforced model for measles and real measles time series, appears to be coincidental.

2000 *Mathematics Subject Classification.* Primary 92D30; Secondary 37N25.

The authors were supported by the Natural Sciences and Engineering Research Council of Canada (NSERC) and an Ontario Premier's Research Excellence Award to D.J.D.E..

1 Introduction

Modelling the population dynamics of infectious diseases is a well-studied problem in mathematical biology due to the implications for public health, the suitability of simple models, and the existence of extensive data sets [9, 12]. A key quantity that models aim to predict is the typical time between epidemic outbreaks. The outbreaks observed in real-world epidemic time series exhibit a wide range of patterns. Outbreaks can be either periodic in time or occur at apparently random times, and periodic outbreaks can be either seasonal (annual, biennial, *etc.*) or non-seasonal.

In epidemic models, attractors (which may or may not be periodic themselves) are often approached by damped oscillations at some natural period. These oscillations can be sustained by demographic stochasticity [2, 6]. The natural period of damped oscillations is, therefore, often used to predict the interepidemic period of real outbreaks of infectious diseases.

The standard model for epidemics of childhood diseases is the SEIR model [2], which divides the population into four compartments according to disease status: S = susceptible, E = exposed but not yet infectious, I = infectious, R = recovered (and immune). Assuming that new exposed (E) cases arise from mass-action mixing among susceptible and infectious individuals, and assuming exponential waiting times for transitions between other compartments, the following system of ordinary differential equations can be derived:

$$\begin{aligned} \dot{S} &= \nu - (\beta I + \mu)S \\ \dot{E} &= \beta SI - (\sigma + \mu)E \\ \dot{I} &= \sigma E - (\gamma + \mu)I \\ \dot{R} &= \gamma I - \mu R \end{aligned} \tag{1.1}$$

Here, ν is the birth rate, μ is the death rate, β is the transmission rate, $1/\sigma$ is the mean latent period (the time between infection and the onset of infectiousness), and $1/\gamma$ is the mean infectious period. We take $\nu = \mu$ throughout this paper, producing a constant population size and reducing the dimensionality of equation (1.1) to three. For simplicity, the transmission rate β is often taken to be constant in time, even when it is known to vary seasonally (as a consequence of the seasonality of school terms). In the following sections, we investigate how this crude approximation of constant β affects the predicted interepidemic interval.

2 The unforced SEIR model

If β is constant then the system of differential equations (1.1) is unforced (autonomous). If the basic reproductive ratio,

$$R_0 = \frac{\beta\sigma}{(\gamma + \mu)(\sigma + \mu)}\,, \tag{2.1}$$

is greater than one, then equations (1.1) have a unique nontrivial stable fixed point (we assume $R_0 > 1$ throughout this paper). There are no asymptotically periodic solutions to this system, but convergence onto the stable fixed point occurs via damped oscillations. The period of these oscillations is determined by the three eigenvalues associated with the linear system obtained by expanding equations (1.1) to first order near the fixed point.

Because $\mu \ll \sigma$ and $\mu \ll \gamma$, one of the three eigenvalues is real, negative and large, and the other two are complex conjugates (see appendix). As a result, orbits collapse rapidly onto a centre manifold and thereafter spiral slowly onto the fixed point [17]. The period of these damped oscillations, T_{u}, is thus determined only by the imaginary part of the complex conjugate pair, and can be written [2]

$$T_{\mathrm{u}} = 2\pi\sqrt{A(1/\sigma + 1/\gamma)}\,. \tag{2.2}$$

Here, A is the mean age at infection, which is related to the birth rate ν and the basic reproductive ratio R_0 via

$$A \simeq \frac{1}{\nu(R_0 - 1)}\,. \tag{2.3}$$

It is the period T_{u} that is normally associated with observed intervals between real epidemics. Oscillations at period T_{u} can be sustained, *i.e.*, convergence onto the fixed point can be prevented, by demographic stochasticity [2, 3, 4, 5, 6, 18]. Anderson and May [1, 2] compare the predicted T_{u} to the observed interepidemic interval for a number of diseases and obtain rough agreement in most cases, with the notable exceptions of chicken pox and rubella.

In the last 20–30 years, it has become clear that seasonal variation in the transmission rate (β) is a crucial factor in the oscillatory behavior of at least some childhood diseases, notably measles (when the time-varying transmission rate is reconstructed from incidence data, the pattern of school terms is readily seen [10, 11]). The amplitude of the seasonal variation of the transmission rate, estimated from real data, is large [10, 11]. It is also known from theoretical work that seasonal forcing of epidemic models induces sustained oscillations [14] at periods different from T_{u}. Thus, in retrospect, it seems paradoxical that T_{u}, the natural period of the unforced model, has good predictive power for the real (forced) system. If seasonal forcing is crucial to the dynamics, how is it that an unforced model can predict the observed interepidemic intervals as well as it does?

3 The seasonally forced SEIR model

To answer this question we analyze the seasonally forced SEIR model, with varying transmission rate specified according to school term dates [8, 15]. Thus we replace the constant parameter β in equation (1.1) with a time varying function $\beta(t)$ that is high on days when school is in session and low otherwise,

$$\beta(t) = \begin{cases} \beta_{\mathrm{H}} & \text{school days,} \\ \beta_{\mathrm{L}} & \text{non-school days.} \end{cases} \tag{3.1}$$

For term dates we use the 2001–2002 academic calendar of the Toronto District School Board: school is in session 4 September to 21 December (*i.e.*, days 247 to 355 of 365), 7 January to 8 March (*i.e.*, days 7 to 67) and 18 March to 27 June (*i.e.*, days 77 to 178). Weekends are counted as low contact days, *i.e.*, $\beta(t) = \beta_{\mathrm{L}}$. These school dates imply that there are a total of 198 school days per year, so the proportion of days in school is

$$p_{\mathrm{s}} = \frac{198}{365} \simeq 0.5425\,. \tag{3.2}$$

The mean transmission rate is

$$\langle\beta\rangle = p_{\mathrm{s}}\beta_{\mathrm{H}} + (1 - p_{\mathrm{s}})\beta_{\mathrm{L}} \tag{3.3}$$

and we define the amplitude of seasonality to be

$$\alpha = \frac{1}{2}\Big(\frac{\beta_{\rm H} - \beta_{\rm L}}{\langle\beta\rangle}\Big)\,. \tag{3.4}$$

In terms of $\langle\beta\rangle$ and α we can write the transmission rate

$$\beta(t) = \begin{cases} \big[(1+2(1-p_{\rm s})\alpha\big]\langle\beta\rangle & \text{school days,} \\ \big[1-2p_{\rm s}\alpha\big]\langle\beta\rangle & \text{non-school days.} \end{cases} \tag{3.5}$$

This form for $\beta(t)$ is more convenient than (3.1) because it is $\langle\beta\rangle$ that corresponds to β in the unforced model (for which $\alpha = 0$). Note that since $\beta(t) \geq 0$, it is clear from equation (3.5) that the range over which the seasonal amplitude α can be varied is

$$0 \leq \alpha \leq \frac{1}{2p_{\rm s}} = \frac{365}{396} \simeq 0.9217\,. \tag{3.6}$$

At the maximum amplitude $\beta_{\rm L} = 0$, *i.e.*, $\beta(t) = 0$ on non-school days.

Just as we can calculate the natural damping period $T_{\rm u}$ of oscillations about the stable fixed point of the unforced model, it is possible to calculate the natural period of damped oscillations onto periodic attractors of the forced model. This can be done using a Poincaré map derived from the forced system of equations, *i.e.*, using the map obtained from the forced system by strobing it once a year (an annual cycle of the full system becomes a fixed point of the map, a biennial cycle becomes a two-cycle, and so on). Then, if the map has fixed points, standard perturbation analysis can be carried out on them to derive the natural period, $T_{{\rm f},1}$, of damped oscillations about annual attractors of the full forced system of differential equations. Similarly, perturbation analysis of n-cycles of the Poincaré map yields the natural period, $T_{{\rm f},n}$, of oscillations near n-year periodic attractors of the full system.

The full forced SEIR equations represent a five-dimensional dynamical system. One variable (typically R) is made redundant by fixing the population size and a second dimension (t) is lost when we focus on the Poincaré map. Consequently, there are three eigenvalues associated with each attractor of the map, as in the unforced case. Away from bifurcation points, the Poincaré map of the forced system has the key property that one of the eigenvalues has small modulus and the other two are complex conjugates. This results in dynamics near the fixed point that are analogous to the dynamics near the stable fixed point of the unforced differential equations; in particular, it can be shown numerically that orbits again collapse quickly onto a centre manifold and thereafter spiral slowly into the fixed point of the Poincaré map. Thus, the epidemiologically interesting information about the interepidemic interval is contained entirely in the complex conjugate pair [7]. As the system approaches the fold bifurcation points, the complex conjugate pair splits, and one of the eigenvalues crosses the unit circle, resulting in the fold bifurcation. However, away from such points the value of $T_{{\rm f},n}$ is given by

$$T_{{\rm f},n} = \frac{2\pi n}{|Arg(\lambda_n)|} \tag{3.7}$$

where λ_n denotes either complex eigenvalue (which, in magnitude, have the same argument).

In Bartlett's classic analysis [6], demographic stochasticity sustains oscillations of period $T_{\rm u}$ about the unforced system's stable fixed point. Similarly, stochasticity

Table 1 Parameters used in this paper. Estimates of R_0 are from Anderson and May [2]. Ranges of $\langle\beta\rangle$ (in years^{-1}) follow from equation (6.3). The disease-independent parameters are always taken to be $\nu = \mu = 0.02$ years^{-1} (as in ref. [8]).

Disease	$1/\sigma$ (days)	$1/\gamma$ (days)	R_0 range	$\langle\beta\rangle$ range
Measles	8	5	5–18	350–1350
Whooping Cough	8	14	10–18	250–500
Rubella	10	7	6–16	300–850
Chicken Pox	10	5	7–12	500–900

may be able to sustain oscillations of period $T_{\mathrm{f},n}$ about the forced system's n-year attractor. This is not certain, however, since the forced system may have multiple coexisting attractors of different periods and stochasticity may cause the system to jump from the basin of one attractor to another [8, 16]; this would be expected to stimulate short-term oscillations at periods $T_{\mathrm{f},n}$ for more than one n, or irregular behaviour if different basins of attraction are densely intermixed. Perturbative analysis of the forced model will predict a single dominant interepidemic period (as with the unforced model) provided there is only one attractor with a substantial basin of attraction; in order to approximate this interepidemic period using the unforced model, it is essential that the dominant attractor of the forced system be the annual cycle that corresponds to the fixed point of the unforced system (the only justification for using T_{u} as an approximation is that $T_{\mathrm{f},1} \to T_{\mathrm{u}}$ as $\alpha \to 0$).

We therefore focus on $T_{\mathrm{f},1}$ and ask how well it is approximated by T_{u}. We end by discussing the circumstances under which $T_{\mathrm{f},1}$ itself should or should not be expected to correspond to the interepidemic interval.

4 Predicted periods in the forced and unforced models

We analyze the Poincaré map of the seasonally forced SEIR model using the bifurcation and continuation software package `Content 1.5` [13]. We study the cases of measles, whooping cough, rubella and chicken pox in figures 1, 2, 3 and 4, respectively. The parameters used to generate these diagrams are listed in table 1, where we have also listed estimates of R_0 and $\langle\beta\rangle$.

In the four diagrams, α ranges from the unforced case at $\alpha = 0$ (where $T_{\mathrm{f},1} = T_{\mathrm{u}}$), to the maximum value given in equation (3.6). In each figure, the top panel shows contours of constant $T_{\mathrm{f},1}$ (in the $\langle\beta\rangle$ vs α plane), and the bottom panel shows contours of constant $\langle\beta\rangle$ (in the $T_{\mathrm{f},1}$ vs α plane). These diagrams make clear how $T_{\mathrm{f},1}$ changes as a function of α.

As can be seen in the bottom panels of the figures, for lower values of $\langle\beta\rangle$ there is little variation in $T_{\mathrm{f},1}$ over the entire range of α. On the other hand, for higher values of $\langle\beta\rangle$, there is moderate change in $T_{\mathrm{f},1}$ as α increases. Thus we see that T_{u} is an excellent approximation to $T_{\mathrm{f},1}$ unless the mean transmission rate $\langle\beta\rangle$ is large. Referring to Table 1, we see that the range of estimated values for $\langle\beta\rangle$ lies in regions where variation in $T_{\mathrm{f},1}$ as a function of α is small. Thus, figures 1 through 4 illustrate the fundamental reason why the unforced natural period T_{u} can roughly predict the observed epidemic intervals of childhood diseases.

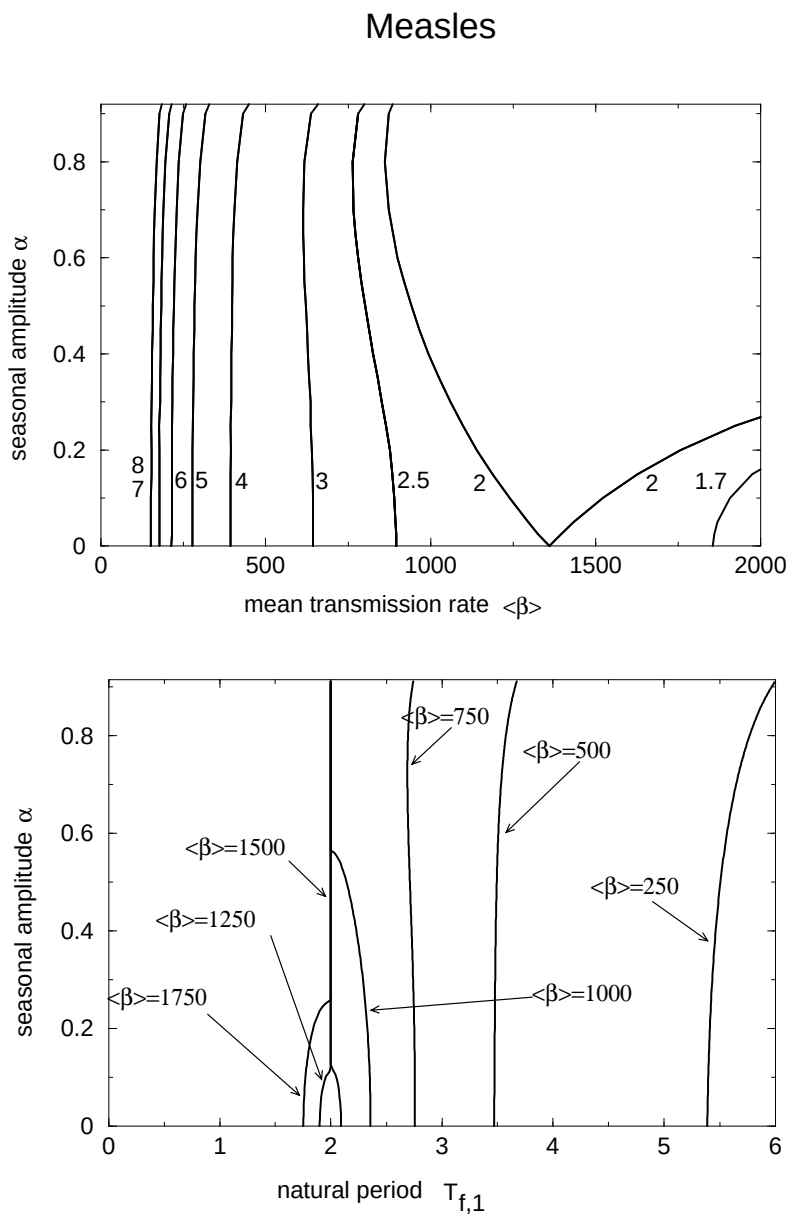

Figure 1 Measles. The top panel shows contours of constant $T_{\mathrm{f},1}$ (the natural period of damped oscillations) in a graph of mean transmission rate $\langle\beta\rangle$ versus seasonal amplitude α. The value of $T_{\mathrm{f},1}$ is indicated next to each contour. $T_{\mathrm{f},1} = 2$ throughout the region between the two $T_{\mathrm{f},1} = 2$ contours. The bottom panel shows contours of constant $\langle\beta\rangle$, in a graph of the natural period $T_{\mathrm{f},1}$ versus α. The value of $\langle\beta\rangle$ is indicated next to each contour. For both panels, the fixed parameters (σ, γ, ν and μ) are specified in Table 1.

5 Discussion

Our numerical analysis in this paper shows that if $T_{\mathrm{f},1}$ correctly predicts the interepidemic period of a typical childhood infectious disease then T_{u} will generally

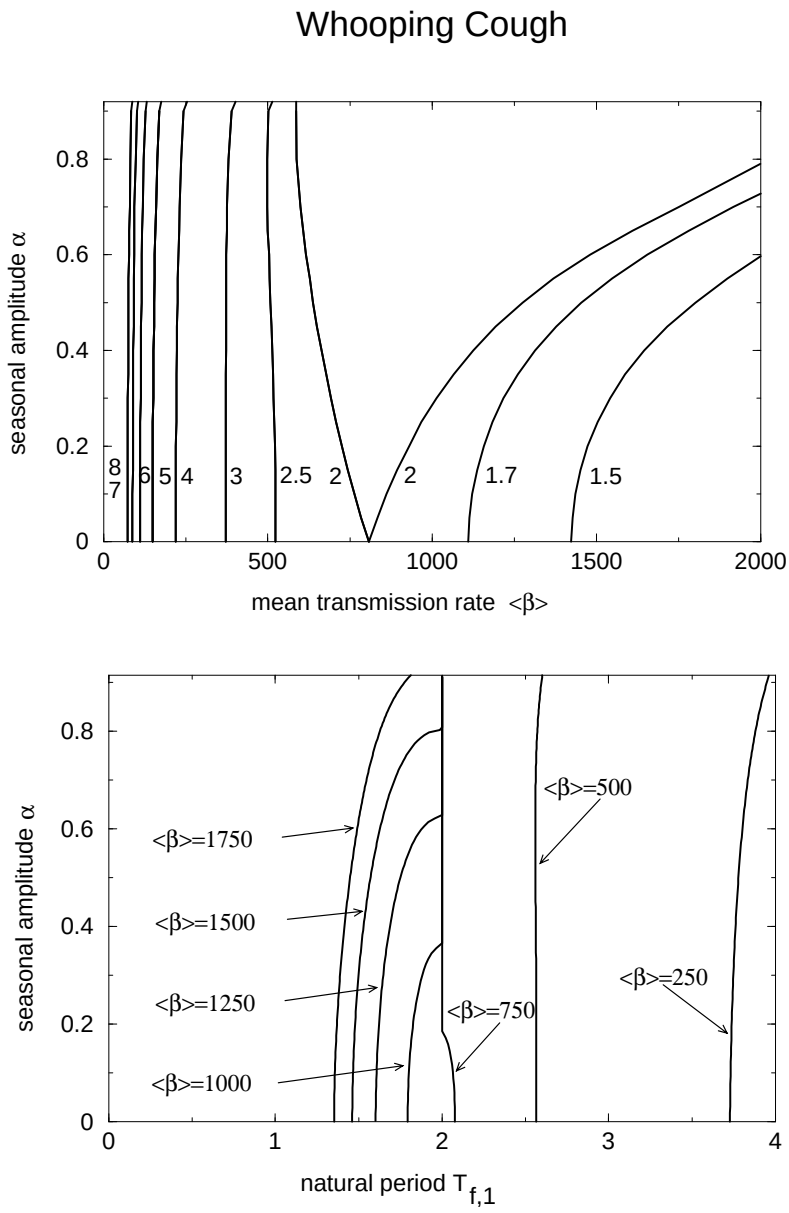

Figure 2 Whooping Cough. See caption to figure 1 for explanation.

do just as well. This provides a justification for previous uses of T_{u} to predict interepidemic intervals. However, as we emphasized at the end of §3, in a seasonally forced system it is not clear that $T_{\mathrm{f},1}$ should have anything to do with the observed interepidemic interval.

A case in point is measles, which in the past was observed to exhibit strictly biennial epidemics over two decades, in both American and British cities [8, 19]. The unforced SEIR model yields $T_{\mathrm{u}} \approx 2$, consistent with $T_{\mathrm{f},1} \approx 2$ in the forced model.

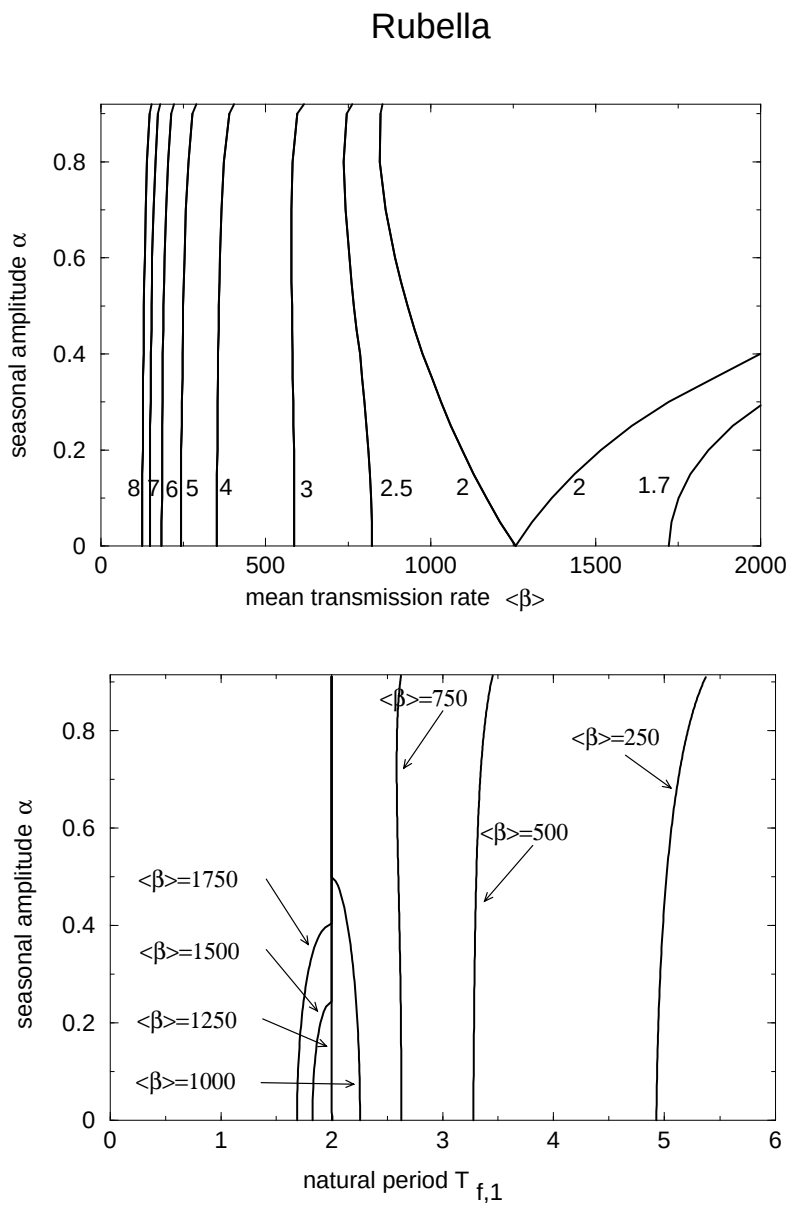

Figure 3 Rubella: See caption to figure 1 for explanation.

However $T_{\mathrm{f},1}$ is an irrelevant quantity in this case because the asymptotically annual cycle of the forced model is unstable. Instead, the transient periodicity must be estimated from the attracting solution, which is itself a biennial cycle. As it happens, the period of oscillation near this attractor is $T_{\mathrm{f},2} \approx 2$. The approximate agreement between T_{u} and the observed interepidemic interval appears to be coincidental. We do not see any justification for using T_{u} to estimate the interepidemic interval in this case.

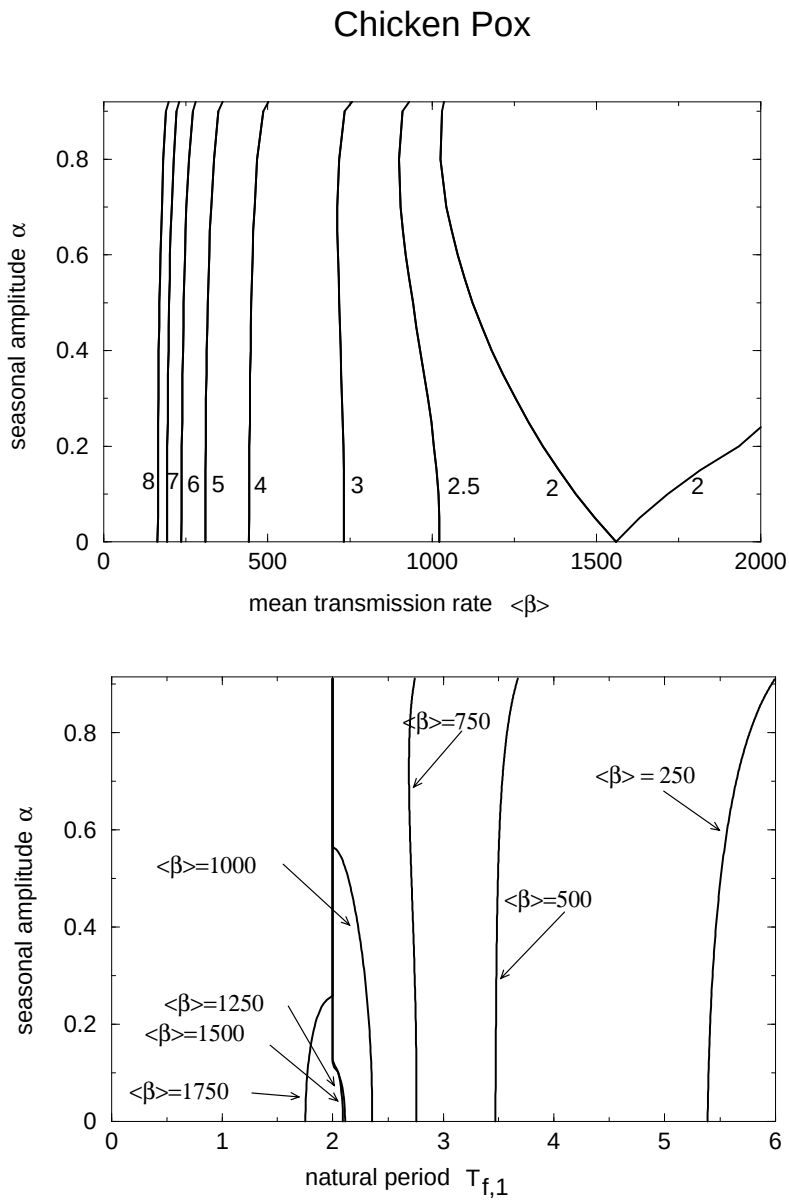

Figure 4 Chicken Pox: See caption to figure 1 for explanation.

More broadly, it is not clear that it makes sense to talk about a single interepidemic period for disease incidence time series. Ideally, we would like to be able to predict the full power spectrum of fluctuations in disease incidence. Many such power spectra show more than one peak, whereas only one peak is expected from analysis of the unforced SEIR model. For example, the power spectrum of rubella in Ontario exhibits both an annual peak and a non-seasonal peak at 5–6 years, whereas the unforced model predicts a single peak at $T_{\mathrm{u}} \approx 4$–5 years. Chicken pox

in Ontario exhibits only a single annual peak, whereas the unforced model predicts a peak at $T_{\rm u} \approx 2$–3 years. A careful analysis of the forced model seems essential to understand this behaviour. Another important issue is to determine how much demographic stochasticity is needed to sustain transients and hence for the analysis of periods of damped oscillations to be relevant to interepidemic intervals. Prediction of interepidemic intervals is further complicated if multiple attractors coexist, which appears to have happened for measles during the Great Depression in the United States and in several countries since the initiation of mass vaccination [8]. We are examining all these issues in greater depth in work in progress [7].

6 Appendix

In this appendix we justify equation (2.2) using the linearization of the SEIR model near its stable fixed point, and a small parameter argument. These results are not new (see, e.g, ref. [17]) but we include them for the sake of clarity and completeness.

The unforced SEIR equations (1.1) with constant population size $\nu = \mu$ reduce to a three-dimensional system,

$$\begin{aligned} \dot{S} &= \mu - (\beta I + \mu) S \\ \dot{E} &= \beta S I - (\sigma + \mu) E \\ \dot{I} &= \sigma E - (\gamma + \mu) I \end{aligned} \tag{6.1}$$

which, for $R_0 > 1$, has the unique nontrivial steady state,

$$S_0 = \frac{1}{R_0}\,, \qquad E_0 = \frac{\mu(R_0-1)(\gamma+\mu)}{\beta\sigma}\,, \qquad I_0 = \frac{\mu(R_0-1)}{\beta}\,. \tag{6.2}$$

Since $\mu \ll \sigma$ and $\mu \ll \gamma$, it follows from equation (2.1) that

$$R_0 \simeq \beta/\gamma\,, \tag{6.3}$$

i.e., the basic reproductive ratio is approximately the product of the mean transmission rate and the mean infectious period.

Since we are interested in the behaviour of the system near the fixed point (S_0, E_0, I_0), it is convenient to introduce new variables (x, y, z) via

$$S = S_0(1+x)\,, \qquad E = E_0(1+y)\,, \qquad I = I_0(1+z)\,. \tag{6.4}$$

The fixed point of interest becomes $(x, y, z) = (0, 0, 0)$ and, to first order in x, y and z, equations (6.1) become

$$\frac{d}{dt}\begin{pmatrix} x \\ y \\ z \end{pmatrix} = \begin{pmatrix} -\mu R_0 & 0 & -\mu(R_0-1) \\ (\sigma+\mu) & -(\sigma+\mu) & (\sigma+\mu) \\ 0 & (\gamma+\mu) & -(\gamma+\mu) \end{pmatrix} \begin{pmatrix} x \\ y \\ z \end{pmatrix} \tag{6.5}$$

The characteristic equation for the matrix above can be written

$$\lambda^2(\lambda+\sigma+\gamma) + \mu\big[(R_0+2)\lambda^2 + (\sigma+\gamma+2\mu)R_0\lambda + (\sigma+\mu)(\gamma+\mu)(R_0-1)\big] = 0\,. \tag{6.6}$$

In the limit $\mu \to 0$, the only non-zero eigenvalue is $\lambda_1 = -(\sigma+\gamma)$. For any μ, exact (but unweildy) expressions for each of the eigenvalues can be derived from equation (6.6). Since μ is small relative to all the other parameters, it is more useful to expand these expressions to leading order in μ. Retaining the leading term for the

real and imaginary parts of each eigenvalue, the three eigenvalues of the matrix in equation (6.5) can be written

$$\begin{aligned} \lambda_1 &= -(\sigma+\gamma) + O(\mu)\,, \\ \lambda_+ &= i\omega\sqrt{\mu} - r\mu + O(\mu^{3/2})\,, \\ \lambda_- &= -i\omega\sqrt{\mu} - r\mu + O(\mu^{3/2})\,, \end{aligned} \tag{6.7}$$

where ω and r can be written

$$r = \frac{1}{2}\left(R_0 - \frac{\sigma\gamma(R_0-1)}{(\sigma+\gamma)^2}\right)\,, \tag{6.8}$$

$$\omega = \sqrt{\frac{R_0-1}{1/\sigma+1/\gamma}}\,. \tag{6.9}$$

Note that $r > 0$ for any parameter values and ω is real and positive if and only if $R_0 > 1$. Thus, since we are assuming $R_0 > 1$, and since $|\lambda_+| \sim |\lambda_-| \ll |\lambda_1|$, near the fixed point we can characterize the behaviour of the system as follows. There is rapid collapse onto a two-dimensional centre manifold at rate $\sigma+\gamma$, followed by oscillations about the fixed point at frequency $\omega\sqrt{\mu}$, which decay slowly at the rate $r\mu$. The period of the damped oscillations is $T_{\rm u} = 2\pi/(\omega\sqrt{\mu})$, as in equation (2.2).

References

[1] Anderson, R.M., B.T. Grenfell, and R.M. May. *Oscillatory fluctuations in the incidence of infectious disease and the impact of vaccination: Time series analysis.* J. Hyg. Camb. **93** (1984), 587–608.

[2] Anderson, R.M. and R.M. May. *Infectious Diseases of Humans*. Oxford Science Publications, OUP, 1991.

[3] Anderson, R.M. and R.M. May. in *Population Dynamics of Infectious Diseases* (eds. Anderson, R.M. and May, R.M.). Chapman & Hall, 1982, pp 1–37.

[4] Anderson, R.M. and R.M. May. in *Population Biology of Infectious Diseases* (eds. Anderson, R.M. and May, R.M.). Springer-Verlag, Berlin, 1982, pp 149–176.

[5] Bailey, N.J.T. *The Mathematical Theory of Infectious Diseases*. Hafner Press, New York, 1975.

[6] Bartlett, M.S. *Measles periodicity and community size.* J. Roy. Stat. Soc. **120** (1957), 48–70.

[7] Bauch, C. and D.J.D. Earn. *in preparation.*

[8] Earn, D.J.D., P. Rohani, B. Bolker, and B.T. Grenfell. *A simple model for complex dynamical transitions in epidemics.* Science **287** (2000), 667–670.

[9] Earn, D.J.D., P. Rohani, and B.T. Grenfell. *Persistence, chaos and synchrony in ecology and epidemiology.* Proc. R. Soc. Lond. B, **265** (1998), 7–10.

[10] Fine, P.E.M. and J.A. Clarkson. *Measles in england and wales–I: An analysis of factors underlying seasonal patterns.* Int. J. Epidemiol. **11** (1982), 5–14.

[11] Finkenstadt, B. and B.T. Grenfell. *Time series modelling of childhood infectious diseases: A dynamical systems approach.* J. Roy. Stat. Soc. C **49** (2000), 187–205.

[12] Grenfell, B.T. and J. Harwood. *(Meta)-population dynamics of infectious diseases.* Trends in Ecology and Evolution **12** (1997), 395–399.

[13] Kuznetsov, Y.A. and V.V. Levitin. Content:a multiplatform environment for continuation and bifurcation analysis of dynamical systems (software under development). Centrum voor Wiskunde en Informatica, Kruislaan 413, 1098 SJ Amsterdam, The Netherlands, 1997.

[14] London, W. and J.A. Yorke. *Recurrent outbreaks of measles, chicken pox and mumps. ii. recurrent outbreaks of measles, chickenpox and mumps.* Am. J. Epidem. **98** (1973), 469–482.

[15] Schenzle, D. *An age-structure model of pre- and post-vaccination measles transmission.* IMA J. Math. Appl. Med. Biol. **1** (1984), 169–191.

[16] Schwartz, I.B. *Multiple stable recurrent outbreaks and preditability in seasonally forced nonlinear epidemic models.* J. Math. Biol. **21** (1985), 347–361.

[17] Schwartz, I.B. and H.L. Smith. *Infinite subharmonic bifurcation in an seir epidemic model.* J. Math. Biol. **18** (1983), 233–253.

[18] Soper. M.A. *The interpretation of periodicity in disease prevalence.* J. Roy. Stat. Soc. **A92** (1929), 34–61.

[19] Yorke, J.A., N. Nathanson, G. Pianigiani, and J. Martin. *Seasonality and the requirements for perpetuation and eradication of viruses in populations.* Am. J. Epidem. **109** (1979), 103–123.